Physical Insights of thin AlGaN Back Barrier for millimeter-wave high voltage AlN/GaN on SiC HEMTs

Ajay Shanbhag, Francois Grandpierron, Kathia Harrouche, Farid Medjdoub

Physical Insights of thin AlGaN Back Barrier for millimeter-wave high voltage AlN/GaN on SiC HEMTs

Ajay Shanbhag,[1] Francois Grandpierron,[2] Kathia Harrouche,[2] and Farid Medjdoub[2]
[1)]*Indian Institute of Technology Madras, India and CNRS-IEMN, Institute of Electronics, Microelectronics and Nanotechnology, Av. Poincare, 59650 Villeneuve d'Ascq, France*
[2)]*CNRS-IEMN, Institute of Electronics, Microelectronics and Nanotechnology, Av. Poincare, 59650 Villeneuve d'Ascq, France*

(Dated: 12 September 2023)

Authors to whom correspondence should be addressed: Ajay Shanbhag, ajay@smail.iitm.ac.in, Farid Medjdoub, farid.medjdoub@iemn.fr

In this work, physical mechanisms underlying carbon-doped buffer combined with an AlGaN back-barrier layer is investigated in state-of-the-art millimeter-wave AlN/GaN transistors. We have fabricated devices with and without the insertion of a thin AlGaN back-barrier layer with reduced carbon concentration to analyze the improvement resulting from this buffer architecture. More specifically, the impact of the Al mole fraction into the back-barrier, carbon doping in the buffer, and channel thickness on 100 nm gate length device performance have been studied. It appears that a 150 nm undoped GaN channel followed by a highly carbon-doped GaN buffer results in good electron confinement at the expense of a high current collapse. On the other hand, an Al mole fraction of 25% in the AlGaN back barrier layer coupled with a 150 nm undoped GaN channel provides excellent electron confinement, resulting not only in a low DIBL under high electric field but also low current collapse. Calibrated on experimental devices, TCAD simulations reveal that the electric field penetration inside the GaN buffer is prevented owing to a strong polarization from the back barrier when the Al-content is high enough. That is why, the electron confinement is superior for the 25% Al mole fraction in the back barrier along with reduced current collapse. As a result, careful engineering of the carbon concentration together with the undoped GaN channel thickness is crucial to achieve robust devices, which can thus deliver high device performance with superior voltage operation while using short gate lengths.

In the last two decades, many reports have shown the capability of Gallium Nitride (GaN) based high electron mobility transistors (HEMTs) to be used for high-frequency power applications[1–20]. In addition, it has been shown that replacing the AlGaN barrier layer with a sub-10 nm AlN barrier can be a potential candidate for millimeter-wave applications due to the availability of higher carrier concentration in the 2-dimensional electron gas (2-DEG) while employing ultra-thin barriers[1]. Hence, AlN/GaN HEMTs with short gate lengths demonstrated state-of-the-art high-frequency power performance[21–23]. However, these applications demand highly robust GaN devices under high bias (e.g. high electric field) while the gate length is shrunk. This, in turn, leads generally to poor electron confinement and high electron trapping due to the large peak electric field. Thus, highly scaled GaN transistors suffer from various secondary effects such as drain-induced barrier lowering (DIBL), current collapse (CC), and self-heating when operated under high drain voltages[1]. Hence, it is necessary to engineer the epitaxial structure and materials to obtain the best performance from the device[1,24,25]. To address this issue, many new structures have been proposed such as carbon-doped (C-doped) GaN buffer[1,25,26], graded channel HEMTs[2,27,28], AlGaN back barrier[24,29], and N-polar HEMTs[3,6,8]. However, each of these designs comes with its own advantages and drawbacks[2,3,5,6]. The most critical issue in all these structures is the limited voltage operation of the short GaN transistors. In this work, we address this issue and show that using a thin AlGaN back barrier layer combined with a C-doped GaN buffer can overcome most of the drawbacks and can be an attractive choice for high-frequency applications with increased voltage operation. We have used TCAD to understand the underlying physical mechanisms improving the device's performance.

In this letter, AlN/GaN HEMTs are fabricated on three different buffer configurations grown on top of a 100 nm AlN nucleation layer using the metal-organic chemical vapor deposition (MOCVD) technique on 4-inch SiC substrates. All three structures have a 150 nm undoped GaN channel with a 3 nm AlN barrier. The device fabrication details are given in[1,24] and the cross-sections are shown in Fig. 1(a), (b), and (c). Device D-1 has a C-doped GaN buffer with a doping concentration of 2×10^{19} cm^{-3} while devices D-2 and D-3 have a 100 nm thick AlGaN back barrier layer (BB) with an Al mole fraction of 10% and 25%, respectively followed by a C-doped GaN buffer of 5×10^{18} cm^{-3}. The AlGaN back barrier has been kept intentionally thin in order to prevent thermal dissipation degradation, especially when using high Al-content[30].The structures are passivated with a 6 nm in situ SiN layer. The gate is defined using e-beam lithography with a length of 100 nm, gate-drain and gate-source distances of 500 nm, and a gate width of 50 µm.

Fig. 1(d), (e), and (f) show the DC characteristic comparison of the three devices. We have used Silvaco Atlas[31] to calibrate these devices in the TCAD framework. We have used the inbuilt polarization model to account for the polarization charges at the interfaces. The drift-diffusion equations are solved numerically using the physical models such as doping and high field dependent mobility models[32], thermionic emission, Shockley–Read–Hall (SRH) recombination, and Fermi statistics. As can be seen in Fig. 1 a satisfactory device cal-

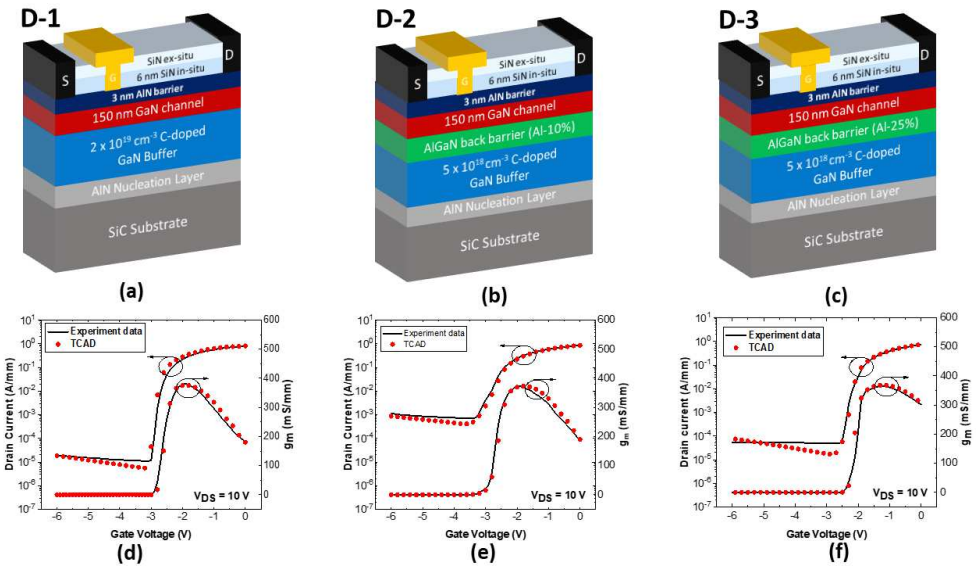

FIG. 1. Cross-sectional view of devices: (a) D-1, (b) D-2, and (c) D-3. Transfer characteristics and transconductance at V_{DS} = 10 V (Experiment vs TCAD) of: (d) D-1, (e) D-2, and (f) D-3 respectively.

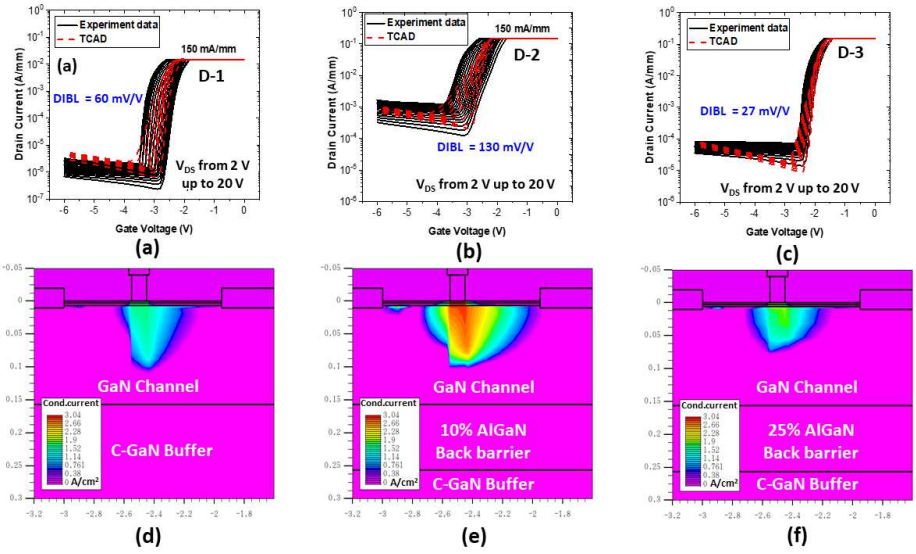

FIG. 2. Transfer characteristics with V_{DS} varying from 2 V to 20 V (Experiment vs TCAD) of: (a) D-1, (b) D-2, and (c) D-3 respectively. Cross-section of the device using TCAD showing the punch-through effect at V_{GS} = -6 V and V_{DS} = 10 V of: (d) D-1, (e) D-2, and (f) D-3 respectively.

TABLE I. TCAD simulated performance metrics with 25% AlGaN back-barrier with varying GaN channel thickness, and GaN buffer carbon concentration.

Buffer C concentration (cm^{-3})	5×10^{18}	2×10^{19}	5×10^{18}	2×10^{19}
GaN channel thickness (nm)	150	150	100	100
DIBL (mV/V)	30	28	27	25
Current Collapse (%)	11.8	14	18.5	19.1
Breakdown Voltage (V)	56	60	103	120

TABLE II. TCAD simulated performance metrics without 25% AlGaN back-barrier by varying GaN channel thickness.

Buffer C concentration (cm^{-3})	2×10^{19}	2×10^{19}
GaN channel thickness (nm)	150	100
DIBL (mV/V)	30	20
Current Collapse (%)	22	40
Breakdown Voltage (V)	58	120

ibration is obtained both in ON-state and OFF-state. Fig. 2 shows the experimental and TCAD results of the transfer characteristics at different drain voltages (V_{DS}) with compliance set at 150 mA/mm. We can see a shift in the threshold voltage as V_{DS} increases, reflecting the DIBL. As seen from Fig. 2(a), (b), and (c) the DIBL is quite large in device D-2, while D-1 and D-3 show an excellent DIBL well below 100 mV/V. To understand this more in-depth, we have simulated the punch-through leakage current under OFF-state with a gate-source voltage (V_{GS}) at -6 V while the V_{DS} is fixed at 20 V as shown in Fig. 2(d), (e), and (f). We observe a significant amount of current flowing through D-2 even under pinch-off conditions as shown in Fig. 2(e). In this case, the back polarization related to the 10% Al content BB is not sufficient to ensure proper electron confinement under such a high electric field, which yields high DIBL. However, in the case of D-1 and D-3, the punch-through leakage current is negligible as shown in Fig. 2(d) and (f). Hence, using a C-doped GaN buffer of 2×10^{19} cm^{-3} or 25% Al content AlGaN back barrier 150 nm away from the 2-DEG is suitable to provide proper electron confinement under a high electric field. C-doped GaN acts as a p-type causing a field opposite to the applied drain field[33,34]. Thus, in the case of D-1, the C-doped GaN layer can prevent field penetration towards the source side, resulting in low DIBL. In the case of D-3, the 25% AlGaN back barrier generates an internal electric field due to the polarization nature of these materials. This internal electric field is in the opposite direction to the applied drain field and consequently prevents the electric field from the drain to affect the source side, resulting also in low DIBL. However, DIBL is not the only factor to be optimized for high-frequency operation. Minimum trapping effects need to be ensured and high breakdown voltages to achieve a high operating voltage device at high frequency.

To assess the trapping effects, pulsed DC characterizations using various quiescent bias points have been carried out. Fig. 3(a) and (b) show the pulsed open channel output drain current characteristics of D-1 and D-3, respectively under cold, gate-lag (V_{GS} = -6 V, V_{DS} = 0 V) and drain-lag (V_{GS} = -6 V, V_{DS} = 20 V) conditions. A significant current collapse is observed in D-1, which is substantially lower in the case of D-3 though in both devices the undoped channel is 150 nm thick. This suggests that the electron trapping is due to the C-doped GaN buffer, which has not only a much higher carbon concentration in D-1 than in D-3 but also is closer to the 2DEG. Furthermore, Table I shows simulations performed on a device similar to the epitaxial structure of D-3 but with various carbon concentrations in GaN buffer. Current collapse, DIBL, and breakdown are thus compared with respect to the different channel thickness / C-doping combinations. It is observed that for an undoped channel thickness of 150 nm, increasing the carbon concentration in the GaN buffer plays no significant role. This implies that the field generated due to the back polarization is sufficient enough to oppose the field due to applied bias, preventing the capture of electrons from the 2-DEG by the deep carbon acceptor traps. Moreover, as we know the current collapse is due to the negative potential developed under pulsing conditions[35], Fig. 3 (c) and (d) show the potential profile within the devices D-1 and D-3. It is clearly visible that the magnitude of the negative potential developed in the case of D-1 in the GaN buffer is much larger than D-3.

Fig. 3(e) and (f) show the vector electric field distribution of D-1 and D-3 in OFF-state (V_{GS} = -6 V) with V_{DS} = 20 V. We can clearly see that the electric field under bias within the GaN buffer is affected, which is reflected by the bent vector lines within the GaN buffer. This indicates that the electric field can penetrate inside the GaN buffer thereby resulting in hot electrons generated under operational conditions that can be trapped. That is why, a C-doped GaN buffer can provide proper field confinement resulting in low DIBL, but high current collapse. However, in the case of D-3, the field lines are all directed upwards due to the presence of the in-built polarization of 25% AlGaN back-barrier. The back barrier confines the electric field and thus prevents its penetration inside the GaN buffer. This results in a reduced current collapse in the case of D-3 up to an extended level of energy as compared to more standard short GaN transistors. Therefore, a thin AlGaN (25% Al) can provide proper electron confinement while preventing the electric field penetration inside the GaN buffer, resulting in both low DIBL and reduced current collapse.

Fig. 4 shows experimental results of continuous-wave (CW) and pulsed large-signal measurements at 40 GHz and V_{DS} = 20 V performed on D-1 and D-2 devices using a nonlinear vector network analyzer. Details of the power bench used for these measurements can be found here[36]. An outstanding power-added efficiency (PAE) is achieved in both

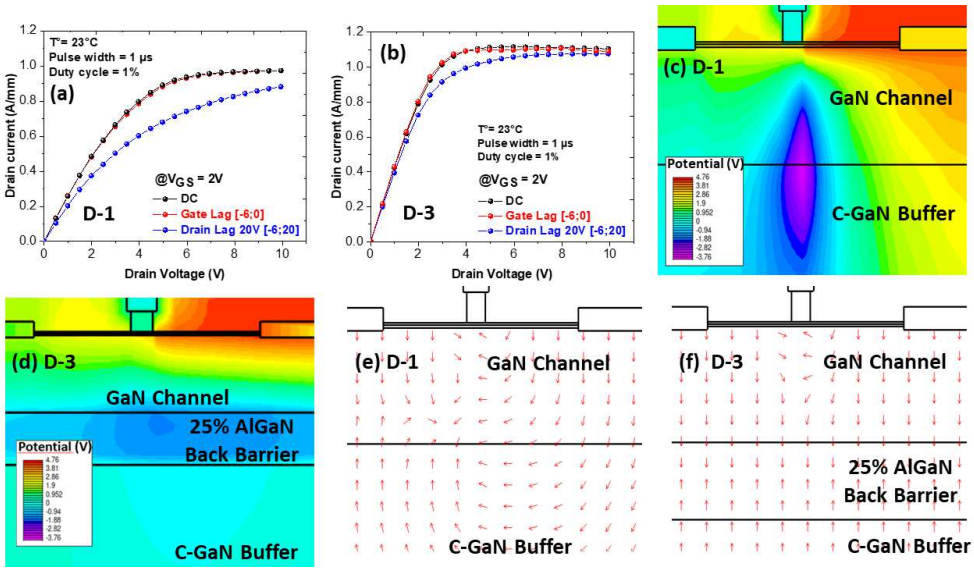

FIG. 3. Pulsed drain current characteristics of: (a) D-1, and (b) D-3. Potential profile using TCAD under pulsed conditions for: (c) D-1, and (d) D-3. TCAD electric field vector distribution (V_{GS} = -6 V and V_{DS} = 20 V) for: (e) D-1, and (f) D-3.

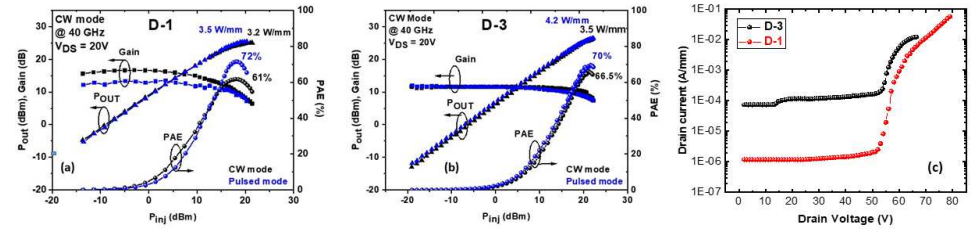

FIG. 4. CW and Pulsed Power Performance at 40 GHz and V_{DS} = 20 V for: (a) D-1 and (b) D-2. (c) Breakdown voltage characteristics for D-1 and D-3.

devices along with a high output power density (P_{OUT}). In addition, the gain of both devices is quite similar for a high range of injected power (P_{inj}). However, Fig. 4(a) shows a large change between CW and pulsed power performance metrics of D-1 unlike D-3 transistors (see Fig. 4(b)) delivering much closer CW / pulsed power performance. This is clearly due to high trapping effects in D-1, which are significantly lower in D-3. This translates the benefit of achieving enhanced electron confinement enabling high-voltage operation together with low trapping effects to achieve superior millimeter-wave large signal characteristics.

Another aspect of high-voltage and high-frequency devices is the breakdown voltage (BV). The measured OFF-state breakdown voltage (drain voltage corresponding to drain current = 1mA/mm) of D-1 and D-3 is 56 V and 60 V respectively as shown in Fig. 4(c). To make the devices more robust, we need to ensure higher BV, which is generally at the expense of trapping effects. Hence, an optimum channel thickness is required to overcome this trade-off. TCAD simulations with reduced channel thickness down to 100 nm and repeating the variation of carbon concentration in the buffer are shown in Table I. As previously described, significant BV improvement of the devices with a reduction in channel thickness is observed. Additionally, a reasonable current collapse penalty is revealed with an increase of only 6%. However, the channel thickness reduction to 100 nm on a device without an AlGaN back-barrier (similar to D-1) results in a current collapse drastically increased to nearly 40% with a BV close to 120 V as shown in Table II. This BV can be achieved using a 100 nm undoped GaN channel followed by a 25% AlGaN back-barrier with C-doped GaN buffer with a carbon concentration of 2×10^{19} cm^{-3}. Fig. 5 shows a benchmark of the results with the proposed structure in comparison to other structures in the millimeter-wave range.

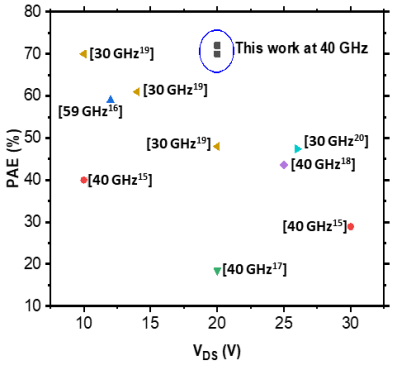

FIG. 5. PAE vs V_{DS} benchmark of GaN HEMTs in the millimeter-wave band.

The performances from the proposed structure are favorably comparable to state-of-the-art GaN HEMTs. In particular, a PAE > 65% combined with a P_{OUT} > 3 W can be achieved.

We demonstrate that a 25% C-doped thin AlGaN back barrier can be an attractive choice to achieve both high electron confinement and reduced trapping effects in short GaN HEMTs. TCAD simulations have shown that the back barrier helps prevent punch-through leakage current and field penetration through the buffer layers. The Al-content into the back-barrier needs to be sufficiently high to generate a proper back polarization that prevents electric field penetration under high bias while reducing the current collapse. The breakdown voltage of the devices can be enhanced by reducing the undoped channel thickness. However, in the case of the absence of a back-barrier, although proper electron confinement can be also achieved, a high current collapse is observed, which is not suitable for power applications. Therefore, we can infer that this device design approach including a 25% thin AlGaN back-barrier can be an optimum choice for high voltage mm-wave applications.

The proposed work was performed under the Raman-Charpak fellowship program partially funded by CEFIPRA and DST as well as the national program LABEX GANEX (ANR-11-LABX-0014) and the French Defense Procurement Agency (DGA) under the project called GREAT. The authors would also like to acknowledge the company SOITEC for high material quality delivery and the support of the French RENATECH network.

The authors have no conflicts to disclose.

The data supporting this study's findings are available from the corresponding authors upon reasonable request.

REFERENCES

[1]K. Harrouche, R. Kabouche, E. Okada, and F. Medjdoub, "High Performance and Highly Robust AlN/GaN HEMTs for Millimeter-Wave Operation," IEEE Journal of the Electron Devices Society **7**, 1145–1150 (2019).
[2]J.-S. Moon, B. Grabar, J. Wong, C. Dao, E. Arkun, H. Tai, D. Fanning, N. C. Miller, M. Elliott, R. Gilbert, N. Venkatesan, and P. Fay, "W-Band Graded-Channel GaN HEMTs With Record 45 % Power-Added-Efficiency at 94 GHz," IEEE Microwave and Wireless Technology Letters **33**, 161–164 (2023).
[3]E. Akso, H. Collins, C. Clymore, W. Li, M. Guidry, B. Romanczyk, C. Wurm, W. Liu, N. Hatui, R. Hamwey, P. Shrestha, S. Keller, and U. K. Mishra, "First Demonstration of Four-Finger N-polar GaN HEMT Exhibiting Record 712-mW Output Power With 31.7 % PAE at 94 GHz," IEEE Microwave and Wireless Technology Letters **33**, 683–686 (2023).
[4]J.-S. Moon, J. Wong, B. Grabar, M. Antcliffe, P. Chen, E. Arkun, I. Khalaf, A. Corrion, J. Chappell, N. Venkatesan, and P. Fay, "360 GHz fMAX Graded-Channel AlGaN/GaN HEMTs for mmW Low-Noise Applications," IEEE Electron Device Letters **41**, 1173–1176 (2020).
[5]Y. Zhou, M. Mi, C. Gong, P. Wang, X. Wen, Y. Chen, J. Liu, M. Yang, M. Zhang, Q. Zhu, X. Ma, and Y. Hao, "High-Efficiency Millimeter-Wave Enhancement-Mode Ultrathin-Barrier AlGaN/GaN Fin-HEMT for Low-Voltage Terminal Applications," IEEE Transactions on Electron Devices , 1–4 (2023).
[6]W. Li, B. Romanczyk, M. Guidry, E. Akso, N. Hatui, C. Wurm, W. Liu, P. Shrestha, H. Collins, C. Clymore, S. Keller, and U. K. Mishra, "Record RF Power Performance at 94 GHz From Millimeter-Wave N-Polar GaN-on-Sapphire Deep-Recess HEMTs," IEEE Transactions on Electron Devices **70**, 2075–2080 (2023).
[7]M. Micovic, D. F. Brown, D. Regan, J. Wong, Y. Tang, F. Herrault, D. Santos, S. D. Burnham, J. Tai, E. Prophet, I. Khalaf, C. McGuire, H. Bracamontes, H. Fung, A. K. Kurdoghlian, and A. Schmitz, "High frequency GaN HEMTs for RF MMIC applications," in *2016 IEEE International Electron Devices Meeting (IEDM)* (2016) pp. 3.3.1–3.3.4.
[8]S. Wienecke, B. Romanczyk, M. Guidry, H. Li, X. Zheng, E. Ahmadi, K. Hestroffer, L. Megalini, S. Keller, and U. K. Mishra, "N-Polar Deep Recess MISHEMTs With Record 2.9 W/mm at 94 GHz," IEEE Electron Device Letters **37**, 713–716 (2016).
[9]D. Marti, S. Tirelli, V. Teppati, L. Lugani, J.-F. Carlin, M. Malinverni, N. Grandjean, and C. R. Bolognesi, "94-GHz Large-Signal Operation of AlInN/GaN High-Electron-Mobility Transistors on Silicon With Regrown Ohmic Contacts," IEEE Electron Device Letters **36**, 17–19 (2015).
[10]B. Romanczyk, X. Zheng, M. Guidry, H. Li, N. Hatui, C. Wurm, A. Krishna, E. Ahmadi, S. Keller, and U. K. Mishra, "W-Band Power Performance of SiN-Passivated N-Polar GaN Deep Recess HEMTs," IEEE Electron Device Letters **41**, 349–352 (2020).
[11]E. Bahat-Treidel, F. Brunner, O. Hilt, E. Cho, J. Wurfl, and G. Trankle, "AlGaN/GaN/GaN:C Back-Barrier HFETs With Breakdown Voltage of Over 1 kV and Low $R_{ON} \times A$," IEEE Transactions on Electron Devices **57**, 3050–3058 (2010).
[12]C. De Santi, E. Zanoni, M. Meneghini, G. Meneghesso, F. Rampazzo, V. G. Zhan, C. Sharma, F. Chiocchetta, G. Verzellesi, A. Chini, *et al.*, "Role of carbon in dynamic effects and reliability of 0.15 um AlGaN/GaN HEMTs for RF power amplifiers," in *Gallium Nitride Materials and Devices XVII*, Vol. 12001 (SPIE, 2022) pp. 92–97.
[13]Z. Gao, F. Chiocchetta, C. De Santi, N. Modolo, F. Rampazzo, M. Meneghini, G. Meneghesso, E. Zanoni, H. Blanck, H. Stieglauer, D. Sommer, L. Benoit, J. Grünenpütt, O. Kordina, J.-T. Chen, J.-C. Jacquet, C. Lacam, and S. Piotrowicz, "Deep level effects and degradation of 0.15 m RF AlGaN/GaN HEMTs with Mono-layer and Bi-layer AlGaN backbarrier," in *2022 IEEE International Reliability Physics Symposium (IRPS)* (2022) pp. P51–1–P51–6.
[14]Z. Gao, F. Rampazzo, M. Meneghini, N. Modolo, C. De Santi, H. Blanck, H. Stieglauer, D. Sommer, J. Grünenpütt, O. Kordina, *et al.*, "Impact of an AlGaN spike in the buffer in 0.15 μm AlGaN/GaN HEMTs during step stress," Microelectronics Reliability **126**, 114318 (2021).
[15]E. Carneiro, S. Rennesson, S. Tamariz, K. Harrouche, F. Semond, and F. Medjdoub, "Low Trapping Effects and High Blocking Voltage in Sub-

Micron-Thick AlN/GaN Millimeter-Wave Transistors Grown by MBE on Silicon Substrate," Electronics **12**, 2974 (2023).
[16]J. Moon, R. Grabar, J. Wong, M. Antcliffe, P. Chen, E. Arkun, I. Khalaf, A. Corrion, J. Chappell, N. Venkatesan, *et al.*, "High-speed graded-channel AlGaN/GaN HEMTs with power added efficiency> 70% at 30 GHz," Electronics Letters **56**, 678–680 (2020).
[17]D. Marti, S. Tirelli, A. R. Alt, J. Roberts, and C. R. Bolognesi, "150-GHz cutoff frequencies and 2-W/mm output power at 40 GHz in a millimeter-wave AlGaN/GaN HEMT technology on silicon," IEEE electron device letters **33**, 1372–1374 (2012).
[18]Y. Zhang, S. Huang, K. Wei, S. Zhang, X. Wang, Y. Zheng, G. Liu, X. Chen, Y. Li, and X. Liu, "Millimeter-wave AlGaN/GaN HEMTs with 43.6% power-added-efficiency at 40 GHz fabricated by atomic layer etching gate recess," IEEE Electron Device Letters **41**, 701–704 (2020).
[19]J.-S. Moon, B. Grabar, J. Wong, D. Chuong, E. Arkun, D. V. Morales, P. Chen, C. Malek, D. Fanning, N. Venkatesan, *et al.*, "Power scaling of graded-channel GaN HEMTs with mini-field-plate T-gate and 156 GHz f T," IEEE Electron Device Letters **42**, 796–799 (2021).
[20]B. Romanczyk, M. Guidry, X. Zheng, P. Shrestha, H. Li, E. Ahmadi, S. Keller, and U. K. Mishra, "Evaluation of linearity at 30 GHz for N-polar GaN deep recess transistors with 10.3 W/mm of output power and 47.4% PAE," Applied Physics Letters **119** (2021), doi.org/10.1063/5.0058587.
[21]A. Hickman, R. Chaudhuri, L. Li, K. Nomoto, S. J. Bader, J. C. M. Hwang, H. G. Xing, and D. Jena, "First RF Power Operation of AlN/GaN/AlN HEMTs With >3 A/mm and 3 W/mm at 10 GHz," IEEE Journal of the Electron Devices Society **9**, 121–124 (2021).
[22]F. Medjdoub, M. Zegaoui, D. Ducatteau, N. Rolland, and P. A. Rolland, "High-Performance Low-Leakage-Current AlN/GaN HEMTs Grown on Silicon Substrate," IEEE Electron Device Letters **32**, 874–876 (2011).
[23]K. D. Chabak, D. E. Walker, M. R. Johnson, A. Crespo, A. M. Dabiran, D. J. Smith, A. M. Wowchak, S. K. Tetlak, M. Kossler, J. K. Gillespie, R. C. Fitch, and M. Trejo, "High-Performance AlN/GaN HEMTs on Sapphire Substrate With an Oxidized Gate Insulator," IEEE Electron Device Letters **32**, 1677–1679 (2011).
[24]K. Harrouche, S. Venkatachalam, L. Ben-Hammou, F. Grandpierron, E. Okada, and F. Medjdoub, "Low Trapping Effects and High Electron Confinement in Short AlN/GaN-On-SiC HEMTs by Means of a Thin AlGaN Back Barrier," Micromachines **14** (2023), 10.3390/mi14020291.
[25]A. Shanbhag, S. M P, F. Medjdoub, A. Chakravorty, N. DasGupta, and A. DasGupta, "Optimized Buffer Stack with Carbon-Doping for Performance Improvement of GaN HEMTs," in *2021 IEEE BiCMOS and Compound Semiconductor Integrated Circuits and Technology Symposium (BCICTS)* (2021) pp. 1–4.
[26]K. Harrouche, R. Kabouche, E. Okada, and F. Medjdoub, "High Power AlN/GaN HEMTs with record power-added-efficiency >70 % at 40 GHz," in *2020 IEEE/MTT-S International Microwave Symposium (IMS)* (2020) pp. 285–288.
[27]J. Moon, S. Wu, D. Wong, I. Milosavljevic, A. Conway, P. Hashimoto, M. Hu, M. Antcliffe, and M. Micovic, "Gate-recessed AlGaN-GaN HEMTs for high-performance millimeter-wave applications," IEEE Electron Device Letters **26**, 348–350 (2005).
[28]J.-S. Moon, B. Grabar, J. Wong, D. Chuong, E. Arkun, D. V. Morales, P. Chen, C. Malek, D. Fanning, N. Venkatesan, and P. Fay, "Power Scaling of Graded-Channel GaN HEMTs With Mini-Field-Plate T-gate and 156 GHz fT," IEEE Electron Device Letters **42**, 796–799 (2021).
[29]F. Medjdoub, M. Zegaoui, B. Grimbert, N. Rolland, and P.-A. Rolland, "Effects of AlGaN back barrier on AlN/GaN-on-silicon high-electron-mobility transistors," Applied Physics Express **4**, 124101 (2011).
[30]J. Tsao, S. Chowdhury, M. Hollis, D. Jena, N. Johnson, K. Jones, R. Kaplar, S. Rajan, C. Van de Walle, E. Bellotti, *et al.*, "Ultrawide-bandgap semiconductors: research opportunities and challenges," Advanced Electronic Materials **4**, 1600501 (2018).
[31]"T.C.A.D. Silvaco, Atlas device user guide." Inc., Mountain View, CA (2022), dOI : `https://silvaco.com/tcad/`.
[32]D. Caughey and R. Thomas, "Carrier mobilities in silicon empirically related to doping and field," Proceedings of the IEEE **55**, 2192–2193 (1967).
[33]M. J. Uren, M. Silvestri, M. Cäsar, G. A. M. Hurkx, J. A. Croon, J. Šonský, and M. Kuball, "Intentionally Carbon-Doped AlGaN/GaN HEMTs: Necessity for Vertical Leakage Paths," IEEE Electron Device Letters **35**, 327–329 (2014).
[34]M. J. Uren, J. Moreke, and M. Kuball, "Buffer Design to Minimize Current Collapse in GaN/AlGaN HFETs," IEEE Transactions on Electron Devices **59**, 3327–3333 (2012).
[35]A. Shanbhag, M. P. Sruthi, A. Chakravorty, N. DasGupta, and A. DasGupta, "Compact Modeling of Static and Transient Effects of Buffer Traps in GaN HEMTs," IEEE Transactions on Electron Devices **69**, 999–1005 (2022).
[36]R. Kabouche, E. Okada, E. Dogmus, A. Linge, M. Zegaoui, and F. Medjdoub, "Power Measurement Setup for On-Wafer Large Signal Characterization Up to Q-Band," IEEE Microwave and Wireless Components Letters **27**, 419–421 (2017).